

Faint K -Selected Galaxy Correlations and Clustering Evolution

R. G. Carlberg,¹ Lennox L. Cowie,^{2,3,4} Antoinette Songaila,^{2,3} and Esther M. Hu^{2,3,4}

ABSTRACT

Angular and spatial correlations are measured for K -band-selected galaxies, 248 having redshifts, 54 with $z > 1$, in two patches of combined area $\simeq 27$ arcmin². The angular correlation for $K \leq 21.5$ mag is $\omega(\theta) \simeq (\theta/1.4 \pm 0.19'' e^{\pm 0.1})^{-0.8}$. From the redshift sample we find that the real-space correlation, calculated with $q_0 = 0.1$, of $M_K \leq -23.5$ mag galaxies (k-corrected) is $\xi(r) = (r/2.9e^{\pm 0.12} h^{-1} \text{ Mpc})^{-1.8}$ at a mean $z \simeq 0.34$, $(r/2.0e^{\pm 0.15} h^{-1} \text{ Mpc})^{-1.8}$ at $z \simeq 0.62$, $(r/1.4e^{\pm 0.15} h^{-1} \text{ Mpc})^{-1.8}$ at $z \simeq 0.97$, and $(r/1.0e^{\pm 0.2} h^{-1} \text{ Mpc})^{-1.8}$ at $z \simeq 1.39$, the last being a formal upper limit for a blue-biased sample. In general, these are more correlated than optically selected samples in the same redshift ranges. Over the interval $0.3 \leq z \leq 0.9$ galaxies with red rest-frame colors, $(U - K)_0 > 2$ AB mag, have $\xi(r) \simeq (r/2.4e^{\pm 0.14} h^{-1} \text{ Mpc})^{-1.8}$ whereas bluer galaxies, which have a mean B of 23.7 mag and mean [O II] equivalent width $W_{eq} = 41 \text{ \AA}$, are very weakly correlated, with $\xi(r) \simeq (r/0.9e^{\pm 0.22} h^{-1} \text{ Mpc})^{-1.8}$. For our measured growth rate of clustering, this blue population, if non-merging, can grow only into a low-redshift population less luminous than $0.4L_*$. The cross-correlation of low- and high-luminosity galaxies at $z \simeq 0.6$ appears to have an excess in the correlation amplitude within $100 h^{-1} \text{ kpc}$. The slow redshift evolution is consistent with these galaxies tracing the mass clustering in low density, $\Omega \simeq 0.2$, relatively unbiased, $\sigma_8 \simeq 0.8$, universe, but cannot yet exclude other possibilities.

¹Department of Astronomy, University of Toronto, Toronto ON, M5S 3H8 Canada
email: carlberg@astro.utoronto.ca

²Institute for Astronomy, University of Hawaii, 2680 Woodlawn Dr., Honolulu, HI 96822
email: acowie, cowie & hu@ifa.hawaii.edu

³Visiting Astronomer, W. M. Keck Observatory, jointly operated by the California Institute of Technology and the University of California.

⁴Visiting Astronomer, Canada-France-Hawaii Telescope, operated by the National Research Council of Canada, the Centre National de la Recherche Scientifique of France, and the University of Hawaii.

1. Introduction

N-body simulations give reliable predictions for the redshift dependence of the two-point correlation function of the density field, $\xi(r|z)$, as a function of Ω . A convenient power-law parameterization to describe the evolving correlation function of galaxies is (Groth & Peebles 1977, Koo & Szalay 1984)

$$\xi(r|z) = \left(\frac{r}{r_0}\right)^{-\gamma} (1+z)^{-(3+\epsilon)}, \quad (1)$$

where the lengths r are measured in physical (proper) co-ordinates. For this double power-law approximation the predicted evolution of clustering in the mass field is faster for $\Omega = 1$ ($\epsilon = 1.0 \pm 0.1$) than it is for low- Ω values, for instance $\epsilon = 0.2 \pm 0.1$ for $\Omega = 0.2$ (Colin, Carlberg & Couchman 1996). Therefore, measurement of the redshift evolution of clustering can be used to test the gravitational instability theory of structure formation and the relation of galaxy clustering to dark matter clustering, and provides a constraint on Ω . Knowledge of these quantities enables predictions of the distribution of assembly times of dark halos, which on the relatively small scales investigated here is of great interest for the mass evolution of galaxies.

At present, observational measures of clustering evolution are uncertain simply due to the difficulties of assembling large samples of faint galaxies with sufficient sky coverage to give a statistically representative sample. At low redshift the form of nonlinear galaxy clustering is accurately established (*e.g.* Davis & Peebles 1983, Loveday *et al.* 1995, Lin 1996, Tucker *et al.* 1996), with a basic characterization of its dependencies on galaxy color, luminosity, and morphology. At higher redshifts the clustering is only now being directly measured (Le Fèvre *et al.* 1996, Shepherd *et al.* 1997), although the small fields leave concerns that field-to-field variations are not yet well controlled.

The galaxy luminosity function and its color dependence evolve substantially over the redshift 0 to 1 interval (Lilly *et al.* 1995, Ellis *et al.* 1996, Cowie *et al.* 1996, Lin *et al.* 1997). Differential luminosity evolution of blue and red galaxies, in which the blue galaxies are less correlated at low redshift, can cause the apparent correlation of a magnitude-limited sample to change faster than either of the two underlying populations are changing. In this paper we report the clustering properties of a very deep redshift survey selected in the K band. A near-IR selected survey has the enormous advantage that both k -corrections and the evolutionary corrections are small, allowing galaxy luminosities to be identified with total stellar mass with reasonable confidence. The Hawaii K -band survey (Cowie *et al.* 1996) with a couple hundred galaxy redshifts, is large enough to be useful for correlation studies. Furthermore this survey contains galaxies up to a redshift of 2.19, which provides a fairly large redshift baseline over which correlation changes can be measured.

The next section summarizes the sample properties. Measures of the angular correlation are given in Section 3 and of the real space correlation function in Section 4. In Section 5 the correlations of red and blue galaxies and of low- and high-luminosity galaxies are compared. Section 6 discusses the redshift evolution of galaxy correlations and compares the available data to various model

predictions. Section 7 summarizes our results. All measurements in this paper assume $H_0 = 100 h^{-1} \text{ km s}^{-1} \text{ Mpc}^{-1}$ and $q_0 = 0.1$. It should be noted that correlation amplitudes at $z \simeq 1$ are reduced by about 30% for $q_0 = 0.5$.

2. The Hawaii K -Band Sample

The Hawaii K -selected redshift survey of two fields constitutes a nearly complete sample down to $K = 20$, $I = 23$, and $B = 24.5$ mag. The survey is described in detail elsewhere (Cowie *et al.* 1996) although this analysis uses 20 new redshifts that have been recently obtained to complete the B selected subsample. The sample of 248 galaxies with redshifts in an area of about 27 square arcminutes compares favourably with the moderate redshift CNOC sample, about 200 galaxies in a single field covering 221 square arcminutes (Shepherd *et al.* 1997), and with the 591 galaxies covering about 71 square arcminutes (a result of the high sampling rate in $0.5' \times 9.4'$ strips) in the CFRS study (LeFèvre *et al.* 1996). On the other hand, the redshifts here extend all the way from 0.08 to 2.19, with 80% between 0.28 and 1.39. The number in any one redshift interval is sufficient to make useful correlation measurements (Figure 1). All magnitudes and colors used in this paper are k -corrected. The sky positions of the objects are plotted in Figure 2, where open squares are galaxies, crosses represent stars, and objects that were not observed or which lack secure redshift identifications are shown with triangles.

The galaxy redshifts, plotted against the projected physical distance in the RA direction from the field center, are shown in Figure 3. The symbol area is proportional to the luminosity of the galaxy. The sample is known to be somewhat incomplete for the redder galaxies at the faintest magnitudes, which are generally expected to be galaxies beyond redshift one with low star formation rates. Incomplete samples, provided that they have no spatial bias, do not pose a problem for correlation studies, provided that the unclustered background distribution is generated from a smoothed version of the observed redshift distribution. We will approximate the observed redshift distributions as being constant over the various subranges of interest, which tests indicate to be an adequate approximation for these data.

3. The Angular Correlation Function

The angular correlation function is estimated as $\omega(\theta) = (DD - 2DR + RR)/RR$ (Landy & Szalay 1993) where in a given range of angles DD is the number of data pairs, DR is the number of pairs between the data sample and a uniform random sample. This estimator is particularly useful when the clustering amplitude is significantly less than unity, as it is here. The resulting angular correlation function for the full photometric sample, $K \leq 21.5$ mag, is shown in Figure 4. The errors are assigned using the bootstrap method (Efron & Tibshirani 1986) with 100 resamplings. The angular galaxy correlations are diluted by the uncorrelated foreground stars, because the full

photometric sample is used, which requires that the correlation amplitude be corrected upward by a factor of $(1 - f_*)^{-2}$, where f_* is the fraction of objects which are stars in the two combined fields. We estimate that $f_* = 0.25$, based on the stellar fraction of the spectroscopically identified sample that are stars. The uncorrected correlation function is $\omega(\theta) \simeq (\theta/0''.75)^{-0.8}$, from which we find that the correlation angle of the galaxies is $\theta_0 = 1''.4 \pm 0''.2$ arcseconds, where the error is the internal error of the fit. Several recent studies in the optical region have found correlation angles of $\theta_0 \simeq 1''$ at $R = 23.5$ mag (Hudon & Lilly 1996), $\theta_0 \simeq 0''.3$ at $I = 22.5$ mag (Lidman & Peterson 1996) and in a much fainter sample to $r = 26$ mag, $\theta_0 \simeq 0''.06$ (Brainerd, Smail & Mould 1995). Since our mean $\langle I - K \rangle \simeq 2.5$ we note that the angular correlation that we observe is substantially larger than for a comparable I - or R -band sample. This is a consequence of the K -band sample's being fundamentally more correlated than optical samples; we provide direct evidence for this below.

In a survey done with a multi-object spectrograph there is the possibility that the angular correlation of the galaxies with redshifts is biased relative to the parent sample as a result of instrumental constraints for the selection of objects for spectroscopy. The simplest test for a selection effect of this type is to measure the ratio of DD pairs as a function of separation in the photometric and redshift sample as normalized to the total numbers in the two samples. We find that there is a 10% reduction in the number of pairs within about $10''$, and a 5% overselection at separations around $30''$, diminishing with increasing angle. This bias is generally less than the statistical errors, so we do not apply any geometric corrections in the correlation measurements.

4. Real Space Correlations

The velocity precision in this redshift survey is not adequate to allow a measurement of the redshift space correlation function at small scales. However, we can measure the projected real space correlation function,

$$w_p(r_p) = \int_{-\infty}^{\infty} \xi(\sqrt{r_p^2 + y^2}) dy, \quad (2)$$

(Peebles 1980, Davis & Peebles 1983). The primary drawback of this estimator is that it averages over long cylindrical shells in redshift space, so it has a very broad window function (Peacock 1996).

The real space correlation is derived from a power-law fit to the projected correlation function, Eq. 2, calculated from the galaxy sample. Operationally, $w_p(r_p)$ is the integral over r_v of the 2D correlation function $\xi(r_p, r_v)$, where r_p and r_v are the proper separation of galaxy pairs in the projected and redshift directions, respectively. Because our sample is not very large the errors are dominated by the small number statistics, rather than any complications of the estimator. We estimate $\xi(r_p, r_v)$ as $DD/DR - 1$, in the (r_p, r_v) co-ordinates. The random sample is 5 to 10×10^4 points. The sum over the r_v co-ordinate is cut off at a practical range of $10h^{-1}$ Mpc in proper co-ordinates at the redshift of the object (Shepherd *et al.* 1997). This value was selected from a range of trial values as being approximately the optimal value to maximize the signal-to-noise. This cutoff distance is sufficiently large that the correction to the integral for the correlation beyond the

cutoff is everywhere less than about 20%, and is ignored. The redshift distribution of the random sample is generated assuming that the unclustered redshift distribution is constant over the various redshift and luminosity ranges. Altering the redshift ranges shows this to be an entirely adequate approximation for these data. The errors are bootstrap estimates, reduced by a factor of $\sqrt{3}$ (Mo, Jing & Börner 1992).

The $w_p(r_p)$ measured over the redshift ranges 0.2–0.4, 0.4–0.8, 0.8–1.2, and 1.2–1.6 are shown in Figure 5. The galaxies have minimum luminosities of $M_K \leq -23.5$ mag in the three higher redshift bins and $M_K \leq -21.5$ in the lower redshift range, to increase the sample size. A rest-frame luminosity of $M_K = -23.5$ mag is about half of L_* .

The $w_p(r_p)$ are fitted to a power-law correlation function,

$$w_p(r_p) = r_0^\gamma \frac{\Gamma(\frac{1}{2})\Gamma(\frac{\gamma-1}{2})}{\Gamma(\frac{\gamma}{2})} r_p^{1-\gamma}, \quad (3)$$

(Peebles 1980). The Gamma function factor is 3.68 for $\gamma = 1.8$. Over the redshift range $0.2 \leq z \leq 0.4$ we find $\xi(r) \simeq (r/2.9e^{\pm 0.12} h^{-1} \text{ Mpc})^{-1.8}$ at a mean $z \simeq 0.34$. For the $0.4 \leq z \leq 0.8$ range we find $\xi(r) \simeq (r/2.0e^{\pm 0.15} h^{-1} \text{ Mpc})^{-1.8}$ at a mean $z \simeq 0.62$, and for $0.8 \leq z \leq 1.2$, $\xi(r) \simeq (r/1.4e^{\pm 0.15} h^{-1} \text{ Mpc})^{-1.8}$ at a mean $z \simeq 0.97$. Using wider projected radius bins we find that for the galaxies with redshifts 1.2–1.6, $\xi(r) \simeq (r/1.0e^{\pm 0.2} h^{-1} \text{ Mpc})^{-1.8}$ at a mean $z \simeq 1.39$. This high redshift correlation is formally an upper limit on the basis of the bootstrap error estimates, although the Poisson errors do indicate a significant measurement. We will accept the result as an indicative measurement, because it remains unclear how best to estimate the errors. The galaxies in this highest redshift bin are dominated by the faint B subsample and are not complete in the K subsample. This selection bias likely leads to an underestimate of the correlation at this redshift if the enhanced correlation of red-selected galaxies over blue-selected ones seen at lower redshift is present at this redshift.

The decrease in the correlation length with increasing redshift is significant within these data although the quoted errors are purely the internal errors of the fit and do not account for field-to-field differences beyond these two patches. The fitted $\epsilon = 0.2 \pm 0.5$, based on our K -band sample alone.

5. Correlation Dependence on Color and Luminosity

The color dependence of faint galaxy clustering is an important clue to the formation mechanisms of galaxies. Higher mass galaxies are expected to be more correlated at formation and subsequently environmental effects can modify the correlations (*e.g.* Loveday *et al.* 1995). In Figure 6 the $w_p(r_p)$ are shown for the $0.3 \leq z \leq 0.9$ galaxies with colors redder or bluer than $(U - K)_0 = 2$ mag (k-corrected, rest-frame ratios between the flux f_ν at 3500\AA and at 21000\AA on the AB magnitude system, see Cowie *et al.* 1996). The red galaxies, with $r_0 = 2.4e^{\pm 0.14} h^{-1} \text{ Mpc}$,

are about 5 times (with about a 50% error) more strongly clustered than the blue objects, which have $r_0 = 0.9e^{\pm 0.22}h^{-1}$ Mpc, both at fixed $\gamma = 1.8$. The red galaxies appear to have a substantially steeper correlation slope, γ , than our adopted value of 1.8, although a survey with larger sky area is needed to assess the slope. The average $M_K = -22.5$ mag for the blue sample, whereas it is $M_K = -23.9$ mag for the red sample, which is quite a small luminosity difference for the large correlation difference (Loveday *et al.* 1995, Tucker *et al.* 1996). The blue population, at a mean B of 23.7 mag, has strong [O II] lines, with a mean W_{eq} of 41Å. Therefore, these are very likely to be substantially brightened relative to their intrinsic luminosities at a more normal star formation rate. The blue galaxy population must largely disappear from the normal galaxy population at low redshift, since its correlation length would grow to only about $2 h^{-1}$ Mpc given our estimated $\epsilon \simeq 0.2$. Within the luminosity range explored in the low redshift APM survey, no population is this weakly correlated (Loveday *et al.* 1995) although the low luminosity, $M_b = -18.6$, late type galaxies have $r_0 = 2.9 \pm 0.4 h^{-1}$ Mpc. We conclude that these high redshift faint blue galaxies cannot become a significant component of the low redshift galaxy population above luminosities of $0.4L_*$. It is possible that these objects merge with higher luminosity galaxies to drive their evolution.

The clustering of lower luminosity galaxies is weaker than that of high luminosity galaxies. For $0.2 \leq z \leq 0.4$ the galaxies with $M_K \geq -21.5$ have $r_0 = 1.8e^{\pm 0.2}h^{-1}$ Mpc and for $0.4 \leq z \leq 0.8$ those with $M_K \geq -23.5$ have $r_0 = 1.1e^{\pm 0.2}h^{-1}$ Mpc. In both these redshift ranges, the higher-luminosity galaxies are more correlated than the lower luminosity ones. The luminosity difference is about 2.5 magnitudes. It is quite unlikely that the high-redshift, high-luminosity, weakly-correlated population could have evolved into a weakly-clustered, low-luminosity, low-redshift population. First, it requires that the clustering is being reduced in physical co-ordinates with time. Second, about 4 magnitudes of fading per unit redshift is required, whereas a much slower rate of luminosity density evolution of the population average is observed (Lilly *et al.* 1995). Third, it would require that the high-luminosity galaxies at lower redshift originate from some unobserved high redshift population — an effect which K -band observations minimize through their relatively small redshift corrections. On the other hand, this discussion does emphasize that a more precise definition of comparable galaxy samples at low and high redshift would be very desirable, ideally done based on the intrinsic properties of the galaxies themselves.

The cross-correlation of low-luminosity galaxies, $M_K \geq -23.5$ mag, with high-luminosity galaxies, $M_K \leq -23.5$ mag, is shown in Figure 7 for the $0.3 \leq z \leq 0.9$ range (expanded slightly to boost the sample size). Although the sample is smaller than is really desirable it shows quite intriguing how much more strongly the low luminosity galaxies cluster to high luminosity “hosts” within $100h^{-1}$ kpc, beyond which the cross-correlation drops to a value similar to the field cross-correlation of low-luminosity galaxies. The effect is directly visible in the redshift diagrams of Figure 3. The enhanced cross-correlation of close pairs is not primarily the result of an enhanced star formation which would raise the optical band luminosity between 1 and 2 magnitudes, and hence would increase the numbers above some flux limit. The lower luminosity galaxies have substantially stronger [O II]; however the expected accompanying increase in the K luminosity is small. Conse-

quently these data favour a genuine increase in close pairs at small separations over the power-law correlation.

6. Evolution of Galaxy Correlations

To follow the clustering amplitude as a function of redshift we need to compare the results of a variety of redshift surveys, having varying r_0 and γ . The quantity r_0^γ , is a useful measure of the clustering amplitude, which can be interpreted either as the amplitude at $1 h^{-1}$ Mpc, or, given that these quantities are normally the results of a fit to data over a range of scales, r_0^γ is a measure of the average correlation within a fixed proper volume.

At low redshift there are several recent measurements of clustering with a range of sample definitions. The b_J -selected APM survey finds $r_0 = 5.1 \pm 0.2 h^{-1}$ Mpc and $\gamma = 1.71 \pm 0.05$ giving $r_0^\gamma = 16.2 \pm 2.5$ at $z \simeq 0.06$ (Loveday *et al.* 1995). The R -selected LCRS finds $r_0 = 5.0 \pm 0.14 h^{-1}$ Mpc and $\gamma = 1.79 \pm 0.04$ giving $r_0^\gamma = 17.8 \pm 2.2$ at a mean $z \simeq 0.1$ (Lin 1996). The IRAS-selected correlation function is $r_0 = 3.76 \pm 0.2 h^{-1}$ Mpc and $\gamma = 1.66 \pm 0.11$ (Fisher *et al.* 1994) for $r_0^\gamma = 9.0 \pm 2.6$. There is no large K -band selected redshift survey at low redshift; however the angular correlation of bright K -selected galaxies is measured, from which we estimate $r_0^\gamma = 27.5$ and 13.8 at $z = 0.13$ and 0.23 , respectively, with $\sim 20\%$ systematic errors (Baugh *et al.* 1996 referred to as BFFS). A preliminary measurement in the LCRS survey finds that the red galaxies have a correlation comparable to these K -band results (Tucker 1994, 1996).

At higher redshift we have the results of this paper, the r -selected CNOC field survey at a mean redshift of 0.36 (Shepherd *et al.* 1997 and work in progress), which gives $r_0^\gamma \simeq 9.6$ for the red half of the sample and 7.5 for the blue half. The CFRS results (LeFèvre *et al.* 1996) provide correlation estimates over the redshift range 0.2 - 0.9 . They find $\xi(r) = (r/2.4 \pm 0.17 h^{-1} \text{ Mpc})^{-1.64}$ for $0.2 \leq z \leq 0.5$, $\xi(r) = (r/1.4 \pm 0.19 h^{-1} \text{ Mpc})^{-1.64}$ for $0.5 \leq z \leq 0.75$, and $\xi(r) = (r/1.4 \pm 0.20 h^{-1} \text{ Mpc})^{-1.64}$ for $0.75 \leq z \leq 1$, where we have adjusted their correlation lengths for $q_0 = 0.5$ to our $q_0 = 0.1$ using their formula. The CFRS data indicate $\gamma = 1.64$, which would be a relatively poor description of the K -selected data here. As a direct comparison with the CFRS measurements, we define a complete subsample limited at $I = 22.5$ mag from our data. We find that $r_0 = 1.9 e^{\pm 0.19} h^{-1}$ Mpc for $0.3 \leq z \leq 0.9$, which is statistically identical to the CFRS measurement of $1.8 \pm 0.18 h^{-1}$ Mpc (adjusted to $q_0 = 0.1$) over the $0 \leq z \leq 1$ range.

The correlation amplitudes are plotted against redshift in Figure 8. For comparison the similarly measured correlations from n-body simulations (Colin, Carlberg & Couchman 1996) are also shown, all scaled with a linear multiplicative factor roughly to fit the LCRS correlation measurement. The fitted γ values from these simulations are in the range 1.8 - 2.0 , which is compatible with the K -band sample but not the shallower slopes usually seen in optically selected samples. The scaling factors are in the range of 0.55 to 0.70 , which is a little larger than desirable (ideally one would do specially matched simulations), however, these factors are small compared to the factor

of 20 or so in the evolution of the correlation functions.

There are two conclusions to be drawn from Figure 8. First, optically selected galaxies appear to always be significantly less correlated than K -selected galaxies, the difference being typically about a factor of two in the amplitude. Second, for the K -band and red-selected samples, which should be least sensitive to galaxy population evolution, we see that the evolution of galaxy clustering is reasonably well described by an $\Omega = 0.2$ model. However, the amplitude measured in the n-body simulation is multiplied by a factor of 0.55, which is approximately the square of the bias factor, $b = 0.75$. Hence, either the galaxies are anti-biased with respect to the matter clustering, or, the normalization of used for the n-body simulations should have been approximately $\sigma_8 \simeq 0.75$. The observed K -band selected evolution appears to be too slow with redshift to readily agree with the $\Omega = 1$ predictions, although the formal level of exclusion is strongly dependent on the low redshift normalization. The second conclusion to be drawn is that the amplitude of the correlations increases as the color used to select the objects becomes redder and there is weak evidence that γ is also steeper in the K sample.

7. Conclusions

The fitted correlation length of luminous K -selected galaxies over the redshift range 0.2 to 1.2 is substantially stronger than that found for optically selected samples, about a factor of two in the amplitude, r_0^γ . The galaxy correlation amplitude is measured at a mean $z \simeq 1.39$ as $r_0 = 1.0e^{\pm 0.2}h^{-1}$ Mpc (formally an upper limit, but deficient in the more strongly clustered faint red galaxies), $r_0 = 1.4e^{\pm 0.15}h^{-1}$ Mpc at $z \simeq 0.97$, $2.0e^{\pm 0.15}h^{-1}$ Mpc at $z \simeq 0.62$, and $2.9e^{\pm 0.12}h^{-1}$ Mpc at $z \simeq 0.34$. Together these give a clustering $\epsilon \simeq 0.2 \pm 0.5$.

The red galaxies are about a factor of 5 more correlated than the blue galaxies, which have $r_0 \simeq 0.9e^{\pm 0.22}h^{-1}$ Mpc. These blue galaxies have a mean equivalent width in the [O II] line of 41Å. Together this can be taken as strong evidence that the faint blue galaxies are an intrinsically weakly correlated population (therefore likely low mass) with a high star formation rate that brightens them into the range of much more strongly correlated red galaxies. These galaxies are so weakly correlated that for our measured growth of correlations, $\epsilon \simeq 0.2 \pm 0.5$, they would grow to a current epoch correlation length of $r_0 \simeq 2h^{-1}$ Mpc. This correlation length is less than that measured in any galaxy population at low redshift (Loveday *et al.* 1995), so these faint blue galaxies cannot by themselves make a significant contribution to the current epoch galaxy population.

Overall the K selected galaxy correlation evolution is somewhat too slow with redshift to be easily consistent with the evolution of the matter correlation function for $\Omega_0 \simeq 1$. A $\sigma_8 \simeq 0.8$ and $\Omega \simeq 0.2 - 0.3$ would describe both the amplitude and its evolution, if these galaxies are tracing the matter clustering. To further test models of correlation evolution requires large datasets of precision comparable to that available in current low redshift surveys with good control over population changes with redshift.

We thank the referee for constructive criticism of an earlier version of this paper. RGC acknowledges the financial support of an NSERC grant. This work was partly based on observations obtained with the NASA/ESA Hubble Space Telescope. Research on the Hawaii Survey fields was supported by the State of Hawaii and by NASA through grants GO-5399.01-93A, GO-5922.01-94A, and GO-6626.01-95A from the Space Telescope Science Institute, which is operated by AURA, Inc., under NASA contract NAS5-26555.

REFERENCES

- Baugh, C. M., Gardner, J. P., Frenk, C. S. & Sharples, R. M. 1996, MNRAS, submitted, (astro-ph/9608142)
- Brainerd, T. G., Smail, I., & Mould, J. R. 1995, MNRAS, 275, 781
- Colin, P., Carlberg, R. G., & Couchman, H. M. P. 1996, ApJ, submitted
- Cowie, L. L., Songaila, A. Hu, E. M., & Cohen, J. G. 1996, AJ, 112, 839
- Davis, M. & Peebles, P. J. E. 1983, ApJ, 267, 465
- Efron, B. & Tibshirani, R. 1986, *Statistical Science*, 1, 54
- Ellis, R. S., Colless, M., Broadhurst, T., Heyl, J., & Glazebrook, K. 1996, MNRAS, 280, 235
- Fisher, K. B., Davis, M., Strauss, M. A., Yahil, A., & Huchra, J. P. 1994, MNRAS, 267, 927
- Groth, E. J. & Peebles, P. J. E. 1977, ApJ, 217, 385
- Hudon, D. & Lilly, S. J. 1996, ApJ, 469, 519
- Koo, D. C. & Szalay, A. S. 1984, ApJ, 282, 390
- Landy, S. D. & Szalay, A. S. 1993, ApJ, 412, 64
- Le Fèvre, O., Hudon, D., Lilly, S. J., Crampton, D., Hammer, F. & Tresse, L. 1996, ApJ, 461, 534
- Lidman, C. E. & Peterson, B. A. 1996, MNRAS, 279, 1357
- Lilly, S. J., Tresse, L., Hammer, F., Crampton, D., & Le Fèvre, O. 1995, ApJ, 455, 108
- Lilly, S. J., Le Fèvre, O., Hammer, F., & Crampton, D. 1996, ApJ, 460, 1L
- Lin, H. 1996, Ph. D. thesis, Harvard University
- Lin, H., Yee, H. K. C., Carlberg, R. G., & Ellingson, E. 1997, ApJ, 475, 494
- Loveday, J., Maddox, S. J., Efstathiou, G., & Peterson, B. A. 1995, ApJ, 442, 457

Mo, H. J., Jing, Y. P. & Börner, G. 1992, *ApJ*, 392, 452

Peacock, J. A. 1996, *MNRAS*, in press (astro-ph/9608151)

Peebles, P. J. E. 1980, *The Large Scale Structure of the Universe*, (Princeton: Princeton University Press)

Shepherd, C. W., Carlberg, R. G., Yee, H. K. C. & Ellingson, E. 1997, *ApJ*, in press

Tucker, D. L. 1994, Ph. D. thesis, Yale University and personal communication

Tucker, D. L., Oemler, A. Jr., Kirshner, R. P., Lin H., Sheckman, S. A., Landy, S. D., Schechter, P. L., Müller, V., Gottlöber, S., and Einasto, J. 1996, *MNRAS*, submitted.

Fig. 1.— The combined redshift distribution of the 248 galaxies with measured redshifts in the B, I, K magnitude-selected sample of the SSA13 and SSA22 fields. The bins have $\Delta z = 0.01$.

Fig. 2.— The positions of K -detected objects on the sky in SSA13 and SSA22. The small ticks are at intervals of $20''$ in RA and $10''$ in Dec. Symbol area is proportional to m_K . Galaxies are shown as squares, stars as crosses, objects without confident redshift identifications as triangles, and unobserved objects as plus signs. A larger fraction of objects in the SSA22 field are stars due to its lower galactic latitude.

Fig. 3.— The redshift vs projected proper distance from field center in the RA direction, calculated for $q_0 = 0.1$ for the entire sample. The area of each circle is proportional to the object’s K -band luminosity. The size for a galaxy with $M_K = -23.5$ is shown near the bottom of the plots at $z = 1.5$.

Fig. 4.— The angular correlation of the photometric sample (including stars). The two points at largest separation have negative values, which are not statistically significant. The indicated 1σ errors are from a bootstrap analysis with 100 resamplings.

Fig. 5.— The projected real space correlation function for redshift subsamples at $0.2 \leq z \leq 0.4$ (top-left panel), $0.4 \leq z \leq 0.8$ (top-right panel), $0.8 \leq z \leq 1.2$ (right panel), and $1.2 \leq z \leq 1.6$. The 1σ bootstrap errors (narrow error flags) indicate that the high redshift correlation is an upper limit, although the Poisson error bars (wide error flags) indicate a significant result. The high redshift subsample is deficient in faint red galaxies, which are expected to be strongly correlated. The point at $0.01h^{-1}$ Mpc corresponds to an angle of about $2''$ where galaxy images overlap and is not used to calculate the correlation length. All errors are from a bootstrap analysis and are considerably larger than Poisson estimates.

Fig. 6.— The projected real space correlation function for the blue and red subsamples over $0.3 \leq z \leq 0.9$. Bootstrap errors are shown.

Fig. 7.— The projected real space cross-correlation function of the $M_K \geq -23.5$ subsample with the $M_K \leq -23.5$ subsample. The line shows the auto-correlation of high luminosity galaxies over the same redshift range. Bootstrap errors are shown.

Fig. 8.— The evolution of the nonlinear amplitude of the correlation function, r_0^γ . The data are compared with results from other surveys in the literature (see Section 6 for details), with all measurements adjusted to $q_0 = 0.1$. The results from this paper are shown as filled circles, with superposed crosses for the blue and red subsamples. The solid, dashed, and dotted lines are based on power law fits to the $\xi(r|z)$ measured in n-body simulations of CDM universes for different assumed values of Ω and Λ , renormalized to pass through the LCRS measurement at low redshift. Note that correlations of relatively red selected galaxies are always larger than those of blue selected galaxies. Bootstrap errors are shown. The Keck and BGFS samples are K selected. CNOG and LCRS are r selected, and CFRS is I selected. The APM is blue selected and the IRAS sample is

dominated by relatively blue galaxies which contain warm dust.

SSA13+22

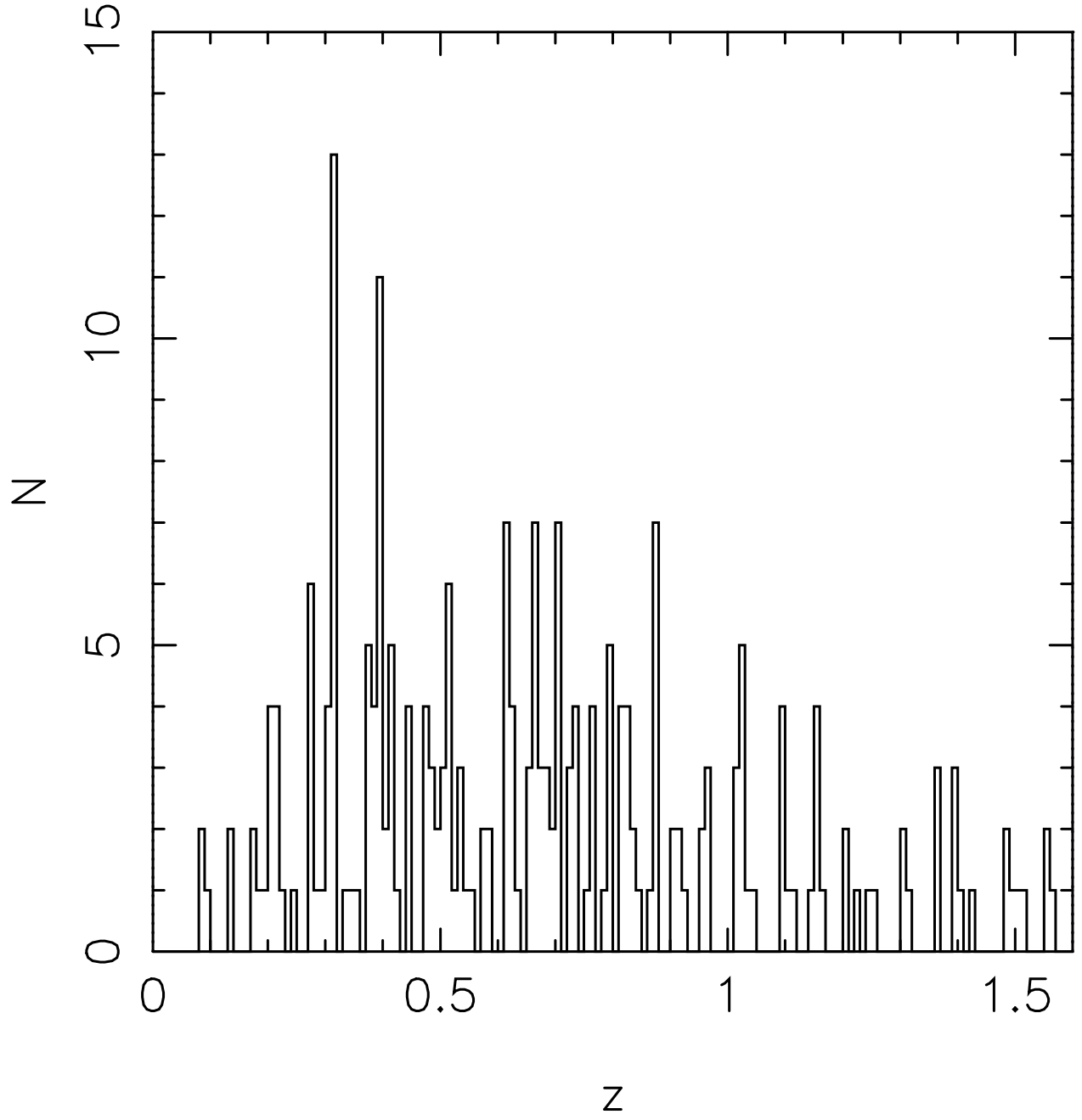


Fig. 1.—

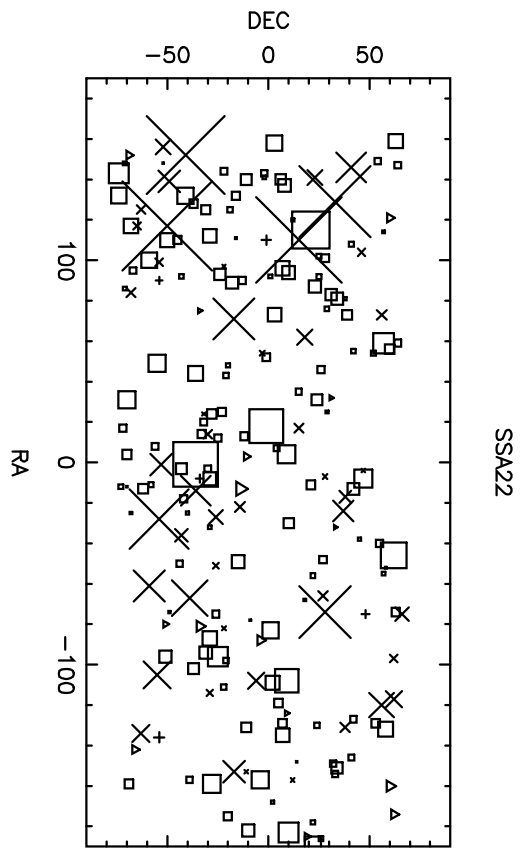
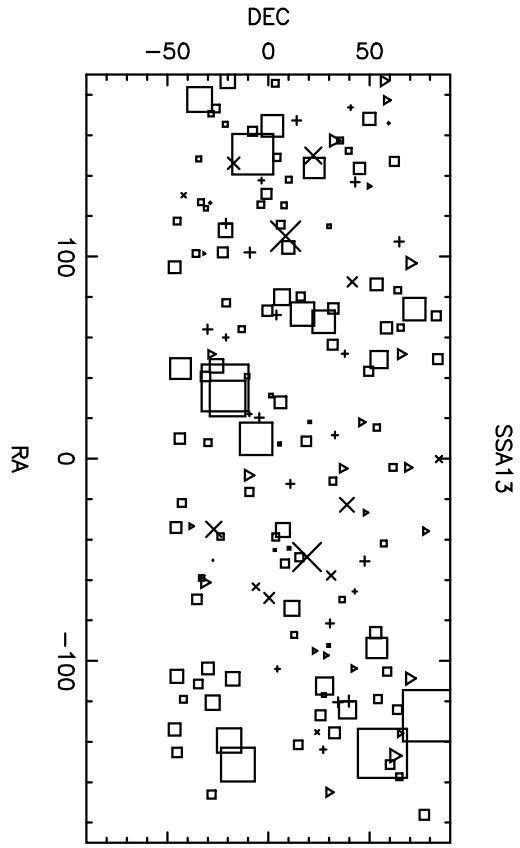


Fig. 2.—

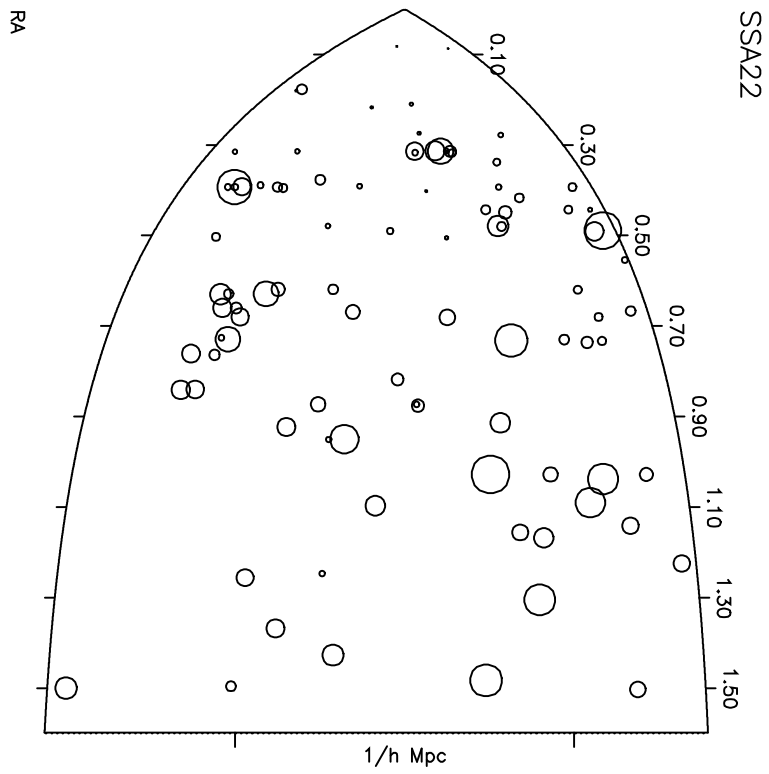
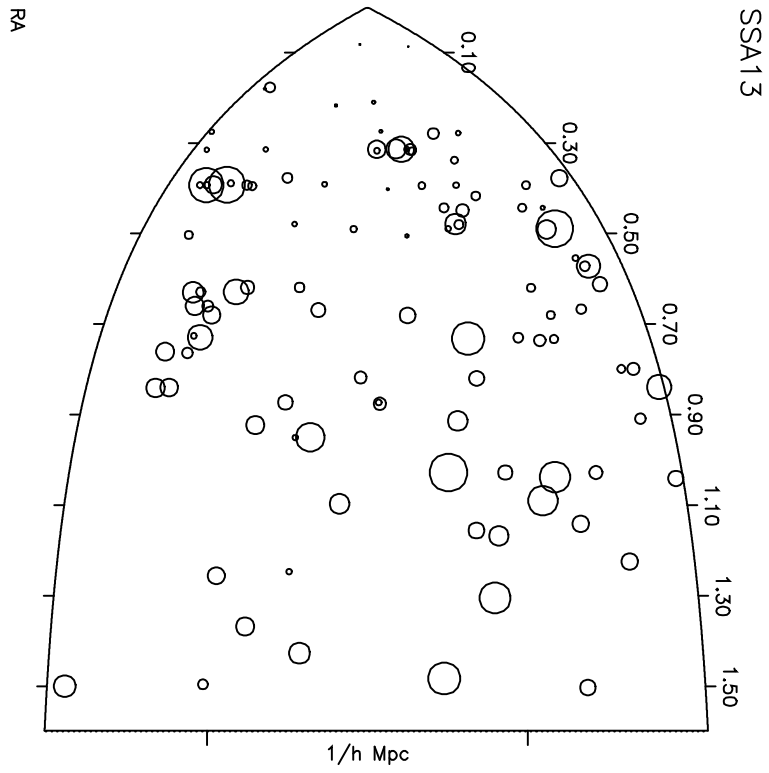


Fig. 3.—

SSA13+22

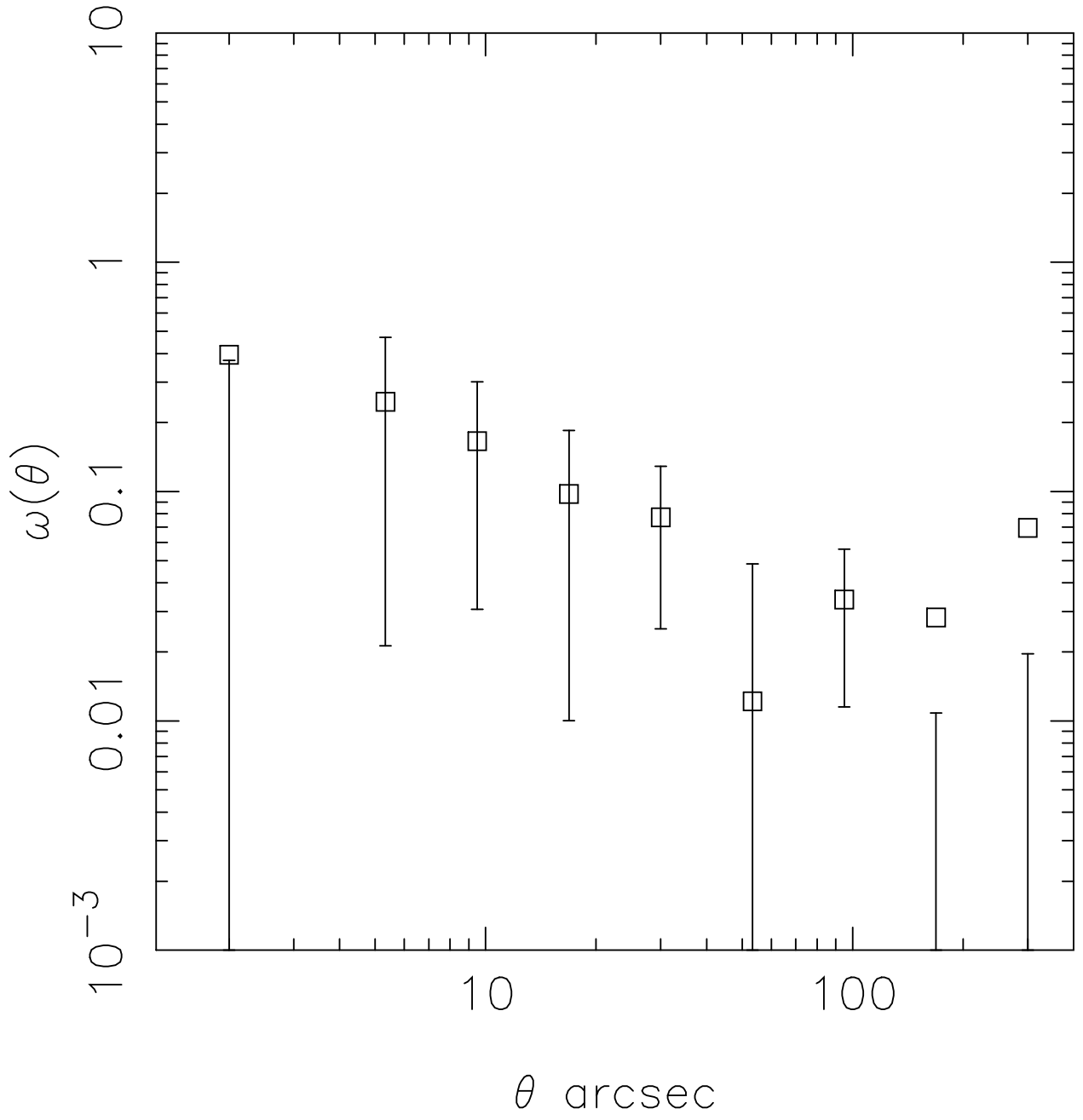


Fig. 4.—

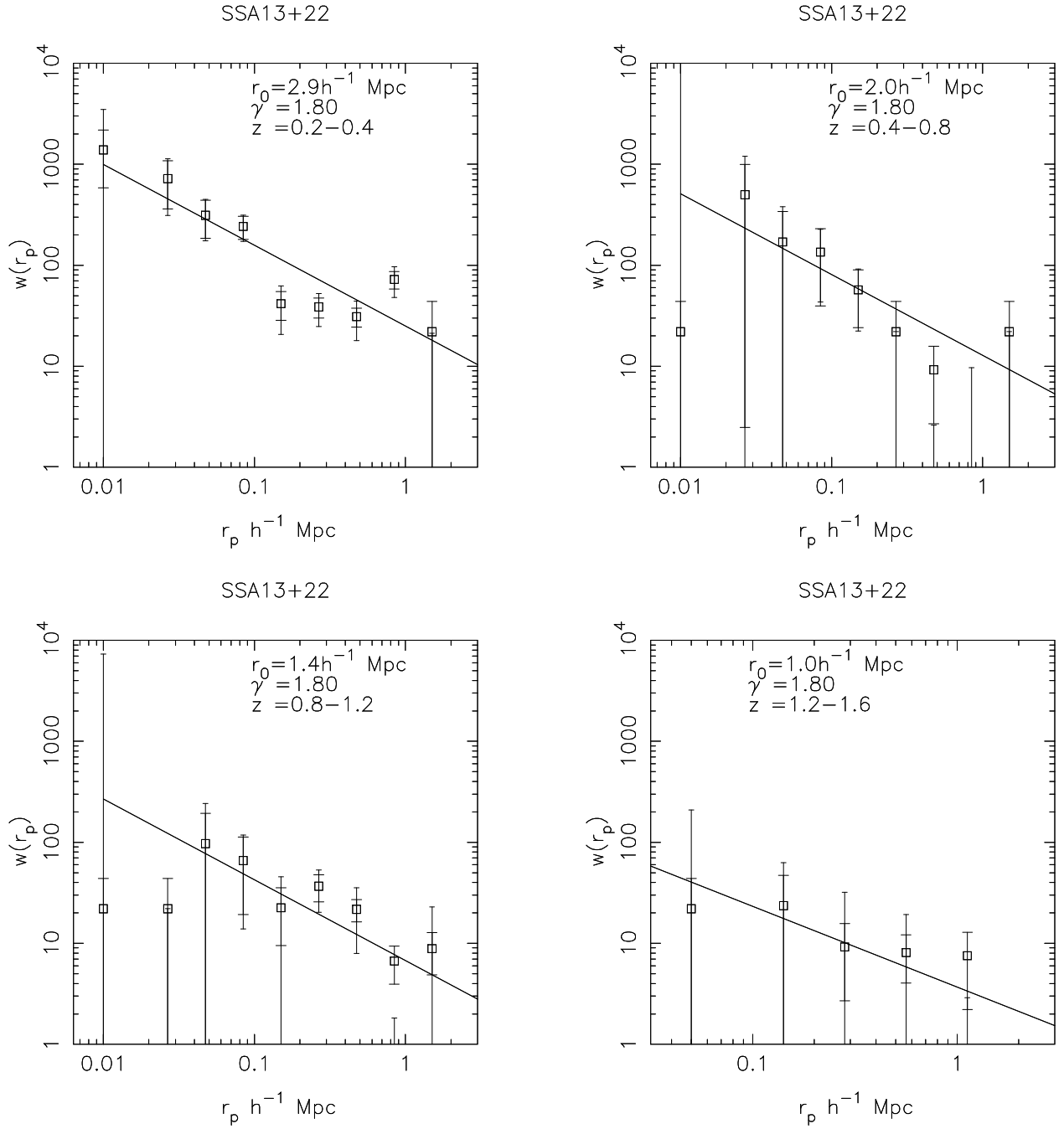


Fig. 5.—

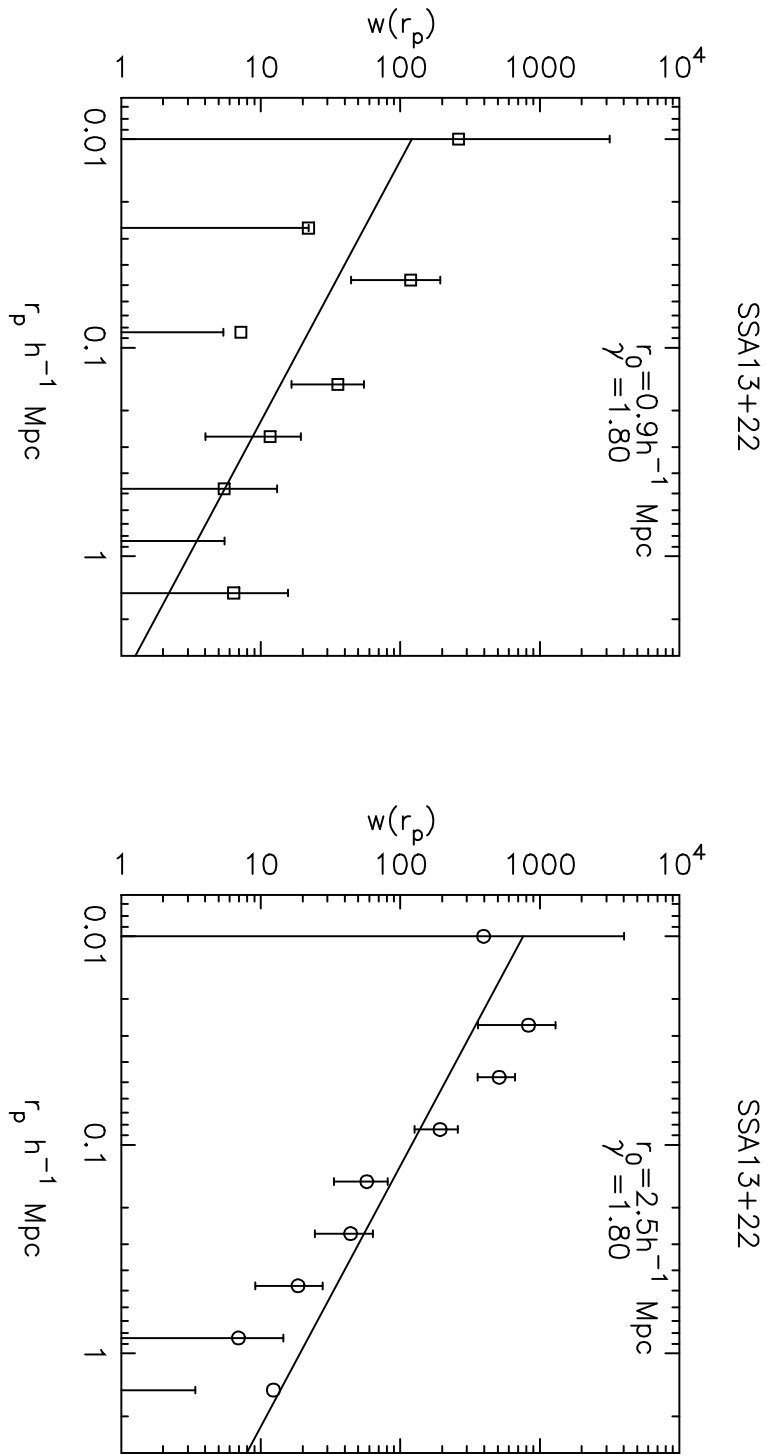


Fig. 6.—

SSA13+22

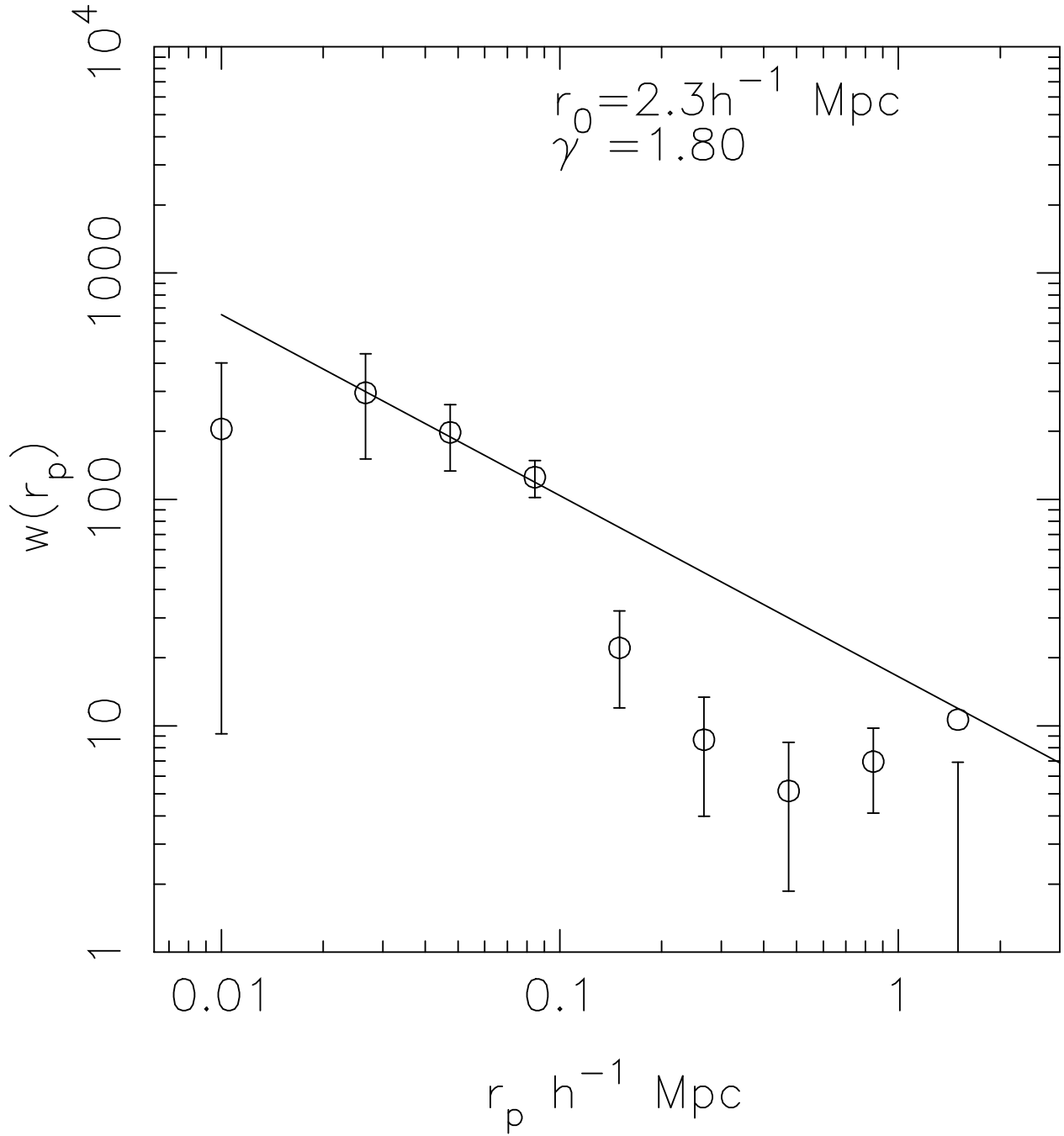


Fig. 7.—

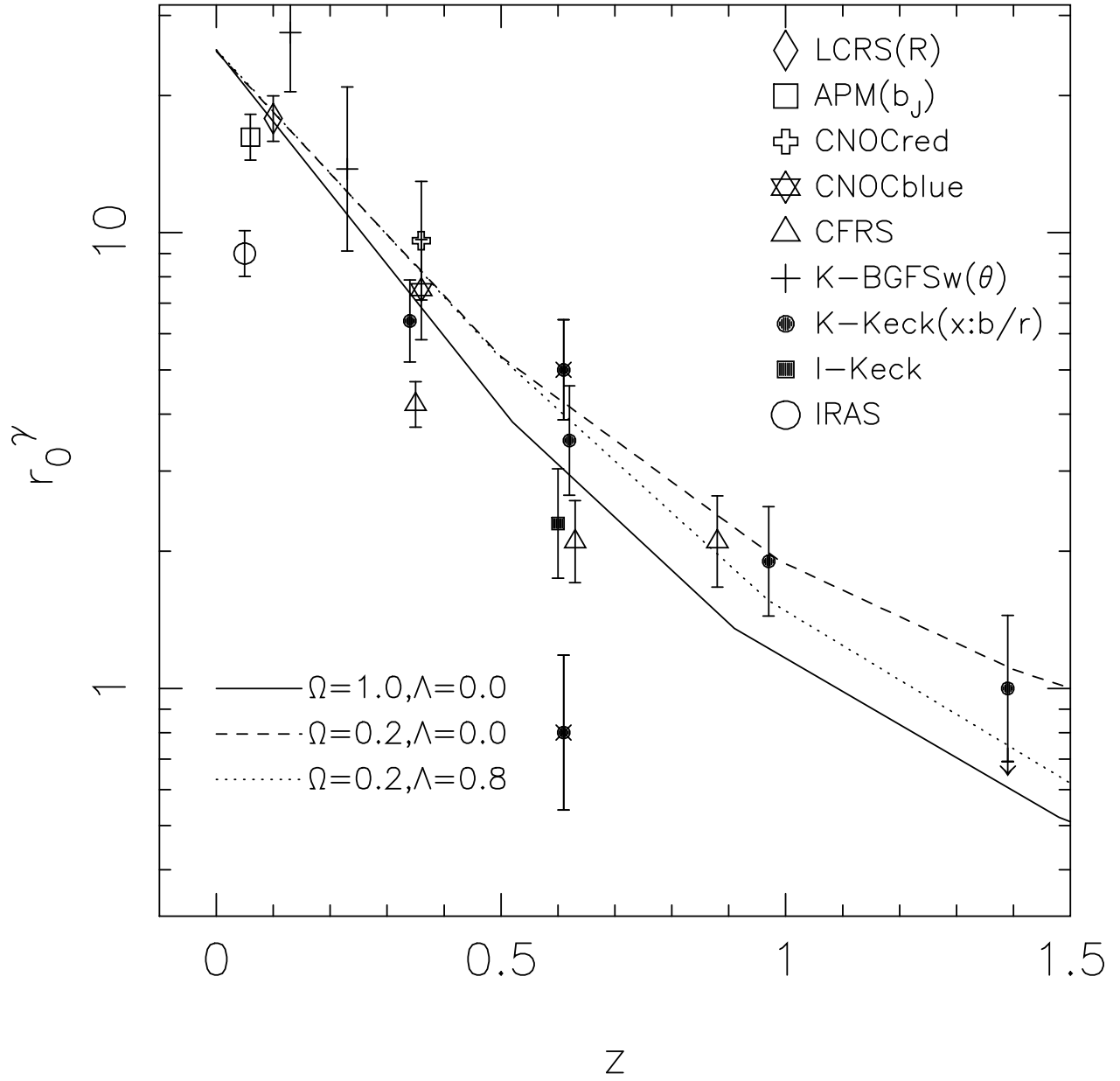


Fig. 8.—